Surg Radiol Anat
DOI 10.1007/s00276-016-1703-0

ORIGINAL ARTICLE

# Morphometric anatomical and CT study of the human adult sacroiliac region

**Roberto Postacchini[1,2] · Guido Trasimeni[3,4] · Francesca Ripani[5] · Pasquale Sessa[5] · Stefano Perotti[6] · Franco Postacchini[5]**

Received: 16 November 2015 / Accepted: 24 May 2016
© Springer-Verlag France 2016

**Abstract**
*Purpose* To identify and describe the morphometry and CT features of the articular and extra-articular portions of the sacroiliac region. The resulting knowledge might help to avoid complications in sacroiliac joint (SIJ) fusion.
*Methods* We analyzed 102 dry hemi-sacra, 80 ilia, and 10 intact pelves and assessed the pelvic computerized tomography (CT) scans of 90 patients, who underwent the examination for conditions not involving the pelvis. We assessed both the posterior aspect of sacrum with regard to the depressions located externally to the lateral sacral crest at the level of the proximal three sacral vertebrae and the posteroinferior aspect of ilium. Coronal and axial CT scans of the SIJ of patients were obtained and the joint space was measured.
*Results* On each side, the sacrum exhibits three bone depressions, not described in anatomic textbooks or studies, facing the medial aspect of the posteroinferior ilium, not yet described in detail. Both structures are extra-articular portions situated posteriorly to the SIJ. Coronal CT scans of patients showing the first three sacral foramens and the interval between sacrum and ilium as a continuous space display only the S1 and S3 portions of SIJ, the intermediate portion being extra-articular. The S2 portion is visible on the most anterior coronal scan. Axial scans show articular and extra-articular portions and features improperly described as anatomic variations.
*Conclusions* Extra-articular portions of the sacroiliac region, not yet described exhaustively, have often been confused with SIJ. Coronal CT scans through the middle part of sacrum, the most used to evaluate degenerative and inflammatory conditions of SIJ, show articular and extra-articular portions of the region.

**Keywords** Anatomy · Sacrum · Ilium · Sacroiliac joint · Extra-articular sacroiliac region · Sacroiliac fusion

✉ Roberto Postacchini
robby1478@hotmail.com

[1] Israelitic Hospital, P. S. Bartolomeo all'Isola 21, Rome, Italy

[2] Department of Movement, Human and Health Sciences, "Foro Italico" University, P. Lauro de Bosis 15, Rome, Italy

[3] Department NESMOS, Section Neuroradiology, Sant'Andrea Hospital, Via di Grottarossa, 1035/39, Rome, Italy

[4] Sapienza University, P. Aldo Moro 5, Rome, Italy

[5] Department of Anatomy, Istology, Legal Medicine and Locomotor Apparatus, Section of Orthopaedic Surgery, Sapienza University, P. Aldo Moro 5, Rome, Italy

[6] Department of Radiology, "Sapienza" University, P. Aldo Moro 5, Rome, Italy

## Introduction

Sacroiliac joint (SIJ) consists of an articular surface present on the lateral aspect of the sacrum and a similar surface on the ilium. These articular portions, which are encircled by a synovial membrane, have a peculiar shape that was compared to an auricle or a crescent [27]. The auricular surface of the sacrum is slightly concave to fit the convexity of homonym surface of the ilium. The latter is surmounted dorsally by the posteroinferior part of the iliac bone.

The sacroiliac region has been the subject of few anatomical studies [14, 15, 20], whereas numerous CT investigations on SIJ were carried out on normal anatomy [29], age-related degenerative changes [4, 7, 8, 12, 25, 28, 32], anatomical variations [4, 6, 19] in asymptomatic subjects, and inflammatory changes in rheumatic conditions [1, 2, 5, 11, 13]. None of these studies specifically dealt with the extra-articular

Published online: 20 June 2016

components of the sacroiliac region. Wheelan and Gold [29] provided a detailed depiction of SIJ in a study on normal CT anatomy of the sacrum, but they focused strictly on the sacral canal and nerve-root foramens, with no mention to SIJ or extra-articular component of the sacroiliac region. Lawson et al. [14], in a study on cadavers and CT scanning of patients with rheumatic sacroiliitis, perceived that the articular portion has different features compared to the extra-articular one. Nonetheless, they made no clear-cut distinction between the two portions in evaluating the pathological changes, which were mostly assessed on coronal CT images.

In performing a CT study on age-related changes of SIJ in asymptomatic subjects, we realized that the coronal scans displaying the joint as a continuous space extending from first to third sacral vertebra, on which many CT studies have assessed the SIJ, include articular and extra-articular components of the sacroiliac region. This perception and the paucity of information on bony anatomy of that region led us to carry out a study on human adult dry sacra, ilia and pelves, to better interpret the findings of the CT study. Our main aim was to provide a correct and exhaustive description of both the bony anatomy and the imaging features of the normal sacroiliac structures. A further purpose was to provide knowledge that might help to decrease the risk of complications when performing SIJ fusion with implants placed across the joint.

## Materials and methods

### Anatomical study

We examined 51 sacra with particular attention to their posterolateral aspect, that exhibits, on both sides, bone depressions that were not described, to the best of our knowledge, in textbooks of anatomy [10, 24, 27] or studies on anatomy of the sacrum [3, 15, 29, 30]. A total of 102 hemisacra could thus be assessed. We measured the height and width (area), depth and anteversion of the depressions. Linear measurements were performed with a horizontal Vernier caliper. Depth was measured using a tipped vertical caliper and anteversion with a compass goniometer. Three types of depressions were identified: oval (Type I), when one dimension (height or width) was greater than the other of at least 5 mm; rectangular (Type II), if the difference between the two dimensions was 2–4 mm; square (Type III), when the two dimensions differed by a maximum of 1 mm. Attention was also paid to the shape and position of the auricular surface with respect to the central part of the sacrum.

Ten intact pelves (iliac bone and sacrum) were examined in the region in which the ilium articulates with the sacrum. Six pelves underwent CT scanning with the same modalities used for patients' examination. In the remaining four, a metallic landmark, consisting of a 3-mm thick copper wire, was introduced in the extra-articular part of the sacroiliac region between ilium and sacrum and CT scanning was performed with the landmark in place. Subsequently, both iliac bones were disconnected from the sacrum to examine the medial aspect of the posteroinferior portion of the 20 ilia. At the end of procedures, the bones were re-connected to the sacrum. Furthermore, 30 right and 30 left isolated iliac bones were evaluated, so that in total 80 ilia were assessed. The bones were obtained from the Institute of Anatomy of "Sapienza" University and the section of Anatomy of "Foro Italico" University, of Rome, Italy; they were obtained from Caucasoid skeletons.

Two examiners, unaware of the design of the study, performed all measurements twice at a distance of 2 weeks. A mean of the values found by each examiner in the two sets of measurement was made. The final figures were the average of the means of the two examiners.

### CT study of patients

The cohort of patients prospectively evaluated consisted of 90 subjects (49 females and 41 males) aged on average 58 years (range 19–82), who underwent CT scanning for diseases not involving the pelvis. Patients with a history of rheumatic conditions, chronic back pain, fractures in the pelvic girdle or a history of previous spine or pelvic girdle surgery were not included in the study. All patients gave their informed consent prior to inclusion in the study. For this type of study, the approval of our IRB is not required.

CT scanning was carried out with a Philips Mx8000 IDT16 apparatus, using volumetric acquisition for abdomen and pelvis (collimation 16 × 1.5, 3-mm slice thickness, increment 3 mm, pitch 1.2, rot time 0.5 s, voltage 120 kV, mAs/slice 190). Raw data were reconstructed in coronal and axial planes: fov 20 cm, contiguous slices 3-mm thick, oriented parallel to major axis of the sacrum for coronal scans and orthogonally to its longitudinal axis for axial scans. For each patient, twenty coronal slices and thirty axial sections were obtained.

Two radiologists assessed, and made measurements on, CT images in consensus. To evaluate the SIJ levels (S1, S2, S3) on axial sections, the synchondroses between each of the upper three sacral vertebral bodies were identified on coronal slices as horizontal lines of bone sclerosis. When the synchondroses were not visible, vertebral bodies were identified based on the site of synchondroses on dry sacra. A horizontal line was traced on the coronal image along the lower part of the first sacral foramens to distinguish the S1 from S2 vertebra, the latter ending at the middle, or lower part, of the second sacral foramens. The S3 vertebral body was identified as that located between the second horizontal line and the lower third of the third sacral foramens.

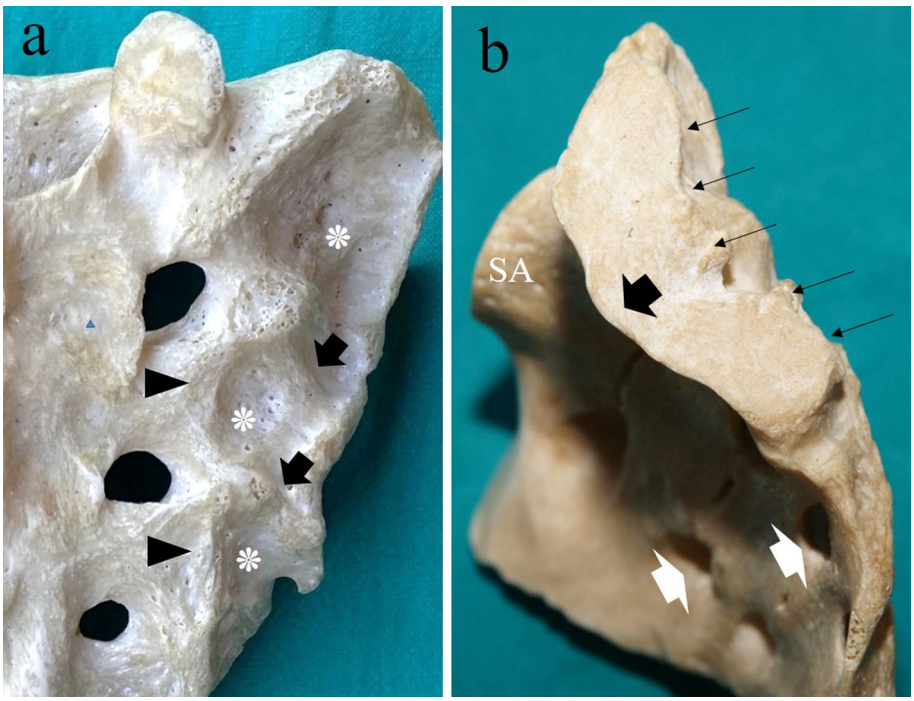


**Fig. 1** **a** Depressions of the posterior aspect of the sacrum (*asterisks*) located externally to the lateral sacral crest (*arrowheads*); the *arrows* indicate the bone prominences separating the three sacral depressions. **b** The auricular surface of the sacrum (*thin arrows*), showing a *crescent* like *shape*, has the central, most prominent, part of the anterior border (*black arrow*) located in *line* with the anterior border of the sacral ala (SA). This part faces the S2 vertebral body and is far apart from the central part of the sacrum; the *white arrows* point to one of the sacral foramens of the two sides

For each vertebra coronal and axial sections were assessed, starting from the anterior to posterior part of the sacrum for coronal images and from the first sacral vertebra downward for axial sections. Measurements were performed using a computer measurement system.

In our cohort of patients, we found all the alterations described in previous studies, such as bone sclerosis, erosions, or subchondral cysts, and their rates were similar to those already reported. Therefore, here we report only the data on the joint space width (JSW), a size below 2 mm being considered the most typical sign of joint degeneration [14]. CT measurements were made at S1, S2 and S3 level on both coronal and axial images. For coronal S1 and S3 levels, measurements were performed on the first coronal scan including the first three sacral foramens and, for the S2 joint space, on the coronal scan tangent to the anterior border of the sacral ala, in which this portion is visible. On each scan, the largest and narrowest joint area were measured and the figures obtained were averaged.

Four groups of patients were identified: Group A (19–35 years), B (36–50), C (51–65) and D (66–81).

### Statistical analysis

The Lilliefors (Kolmogorov–Smirnov) normality test was performed for the assessed variables. All showed a normal distribution, Mean and standard deviation (SD) were computed for all measurement sets. Paired *T*-tests were performed to assess differences between means of right and left side of dry sacra. The level of significance was set at 0.05. SPSS for Windows (version 17.0, SPSS, Chicago, IL) was used for statistical analysis.

## Results

### Anatomy of sacrum

The bone depressions on the posterior aspect of sacrum correspond to the spaces between two contiguous transverse processes in the lumbar spine. They are located laterally to the lateral sacral crest and posteriorly to the auricular surface of the sacrum (Fig. 1a). The cranial depression, the largest one, is situated along the entire S1 vertebra and proximal half, or entire, first sacral foramen. The middle depression is located at the level of the S2 vertebra and almost consistently of proximal part of the second sacral foramen. The caudal depression, the smallest one, is often vestigial or absent. When present, it is located between the second and third sacral foramen. The cranial and middle depressions are consistently separated by a bone prominence of varying width and height, whereas the bone crest between the middle and caudal depression is usually thin and often incomplete or absent (Fig. 1a).

The depressions exhibited variable width and height (area), depth and anteversion in different sacra or on the two sides of a single bone. Nevertheless, the mean area, depth and anteversion did not change significantly between right and left side of a single site (Table 1). Conversely, significant differences were found between sites. When

**Table 1** Data on anatomic features of sacral depressions

| Type *N* (%) | Area ($cm^2$) Mean ± SD | Depth (cm) Mean ± SD | Anteversion Mean ± SD |
|---|---|---|---|
| Cra Rt | | | |
| I 31 (60.7) | | | |
| II 13 (25.4) | 3.36 ± 0.97 | 0.67 ± 0.26 | 47.8 ± 6.6 |
| III 7 (13.7) | | | |
| Cra Lt | | | |
| I 29 (56.8) | | | |
| II 17 (33.3) | 3.58 ± 1.16 | 0.73 ± 0.32 | 44.3 ± 8.15 |
| III 5 (9.8) | | | |
| Mid Rt | | | |
| I 17 (33.3) | | | |
| II 24 (47.0) | 2.88 ± 1.24 | 0.55 ± 0.23 | 42.1 ± 9.8 |
| III 10 (19.6) | | | |
| Mid Lt | | | |
| I 17 (33.3) | | | |
| II 24 (47.0) | 2.65 ± 1.25 | 0.56 ± 0.14 | 41.7 ± 7.71 |
| III 10 (19.6) | | | |
| Cau Rt | | | |
| I 7 (15.9) | | | |
| II 15 (34.0) | 0.85 ± 0.57 | 0.31 ± 0.29 | 38.1 ± 11.3 |
| III 22 (50.0) | | | |
| Cau Lt | | | |
| I 5 (11.6) | | | |
| II 13 (30.2) | 0.95 ± 0.54 | 0.33 ± 0.12 | 36.0 ± 12.3 |
| III 25 (58.1) | | | |

The total number of caudal depressions assessed was 87 since the depression could not be identified on both sides in seven sacra and on the left side in one sacrum

*SD* standard deviation, *Cra* cranial, *Mid* middle, *Cau* caudal, *Rt* right side, *Lt* left side

comparing the mean area or depth of both sides taken together, the values of the cranial depression were significantly greater than those of middle ($p = 0.009$ and 0.005, respectively) or caudal depression ($p = 0.001$ and 0.001) and those of the middle greater than those of caudal one ($p = 0.001$ and 0.002). A significant difference was found for anteversion between cranial and caudal depressions ($p = 0.009$). Type I depression prevailed in cranial, Type II in middle and Type III in caudal site (Table 1).

In 58 % of sacra, the auricular surface had a crescent-like shape, consisting of a proximal portion directed from back to front and a caudal portion of approximately the same size exhibiting an opposite direction (Fig. 1b). In 42 %, the auricular surface showed a L-shape because, below a cranial crescent-like part, the joint continued distally in a vertical direction to reach the lowermost part of S2, or the uppermost portion of S3, vertebra.

Regardless of the shape, the center of the crescent-like part, representing the most medial border of the articular plane, is prominent ventrally and tangent to the anterior border of the sacral ala. This portion, corresponding to the upper and/or middle part of the S2 vertebra, is thus situated at a distance from the central region of sacrum, which is located between the sacral foramens of the two sides (Fig. 1b).

## Anatomy of ilium

The medial aspect of the posteroinferior part of the ilium displays, approximately 2 cm below the posterior iliac spine, a small bone prominence (Fig. 2a), which articulates with the most cranial and lateral part of the sacral ala. Distally to it, a narrow, smooth depression is visible, the inferior border of which represents the limit of the iliac auricular surface. Proximally to that depression there is a large bone prominence so-called "iliac tuberosity", which is roundish or slightly rectangular in shape, with the central, most prominent, part facing the center of the iliac auricular surface (Fig. 2a). Cranially, the prominence abuts on a large area of wrinkly bone that ascends to reach the iliac crest.

When the ilium is re-connected to sacrum, the most prominent part of the iliac tuberosity is in close contact with the bone prominence separating the cranial and middle sacral depressions. As a result, a space of variable size is present between iliac bone and each of those depressions (Fig. 2b). The spaces are occupied in vivo by posterior sacroiliac ligaments.

The height and width of the large iliac prominences were measured at their central point in the 80 ilia. For the height, the mean (±SD) of the measurements of the two examiners was 1.51 cm (±0.23) on the right side and 1.60 cm (±0.21) on the left side, the difference being significant ($p = 0.001$). The mean width was 2.04 cm (±0.45) on the right and 2.05 cm (±0.47) on the left, with no significant difference between the two sides. The intra- and inter-examiner reliability were 0.92 (95 % CI 0.85–0.96) and 0.90 (95 % CI 0.89–0.93), respectively.

## CT scanning of pelves with landmark

All structures described above are located posteriorly to SIJ, contiguous to, but independent from, it. This was confirmed by the position of the copper wire introduced into the lowermost part of the cranial space between ilium and sacrum and pushed distally (Fig. 3a). The axial CT scan obtained with the landmark on site showed that the wire was outside the SIJ, posteriorly to the S1 portion of the joint (Fig. 3b).

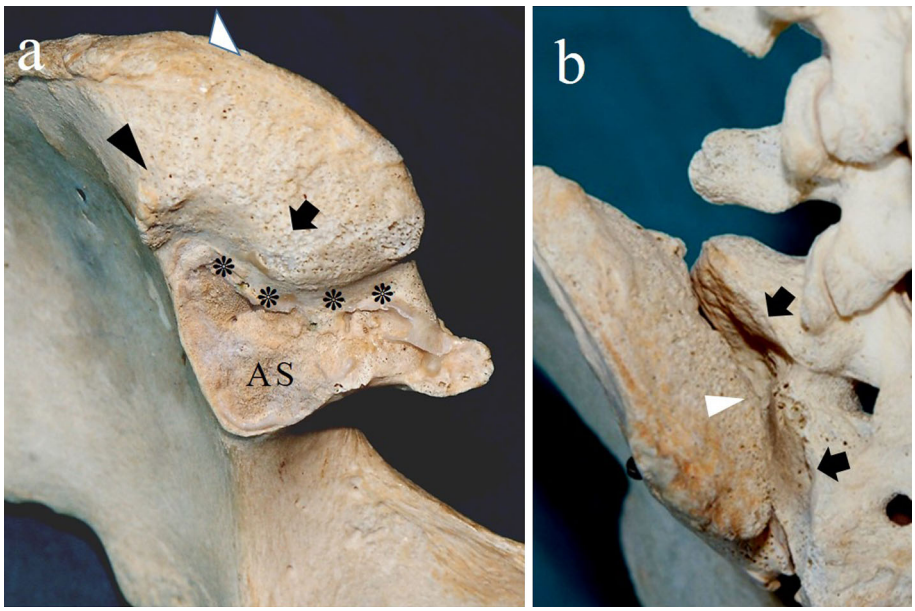


**Fig. 2** **a** Medial aspect of the posteroinferior portion of the ilium showing a small prominence (*black arrowhead*) located inferiorly to the posterosuperior iliac spine (*white arrowhead*), a smooth bone depression (*asterisks*) separating the auricular surface of the ilium (AS) from a roundish bone prominence (*large arrow*) which faces the center of the auricular surface. **b** Posterior aspect of extra-articular junction between ilium and sacrum. The presence of the central bone prominence (*arrowhead*) separates the cranial and middle sacral depressions leaving *empty spaces* (*arrows*) between the surfaces of sacrum and ilium

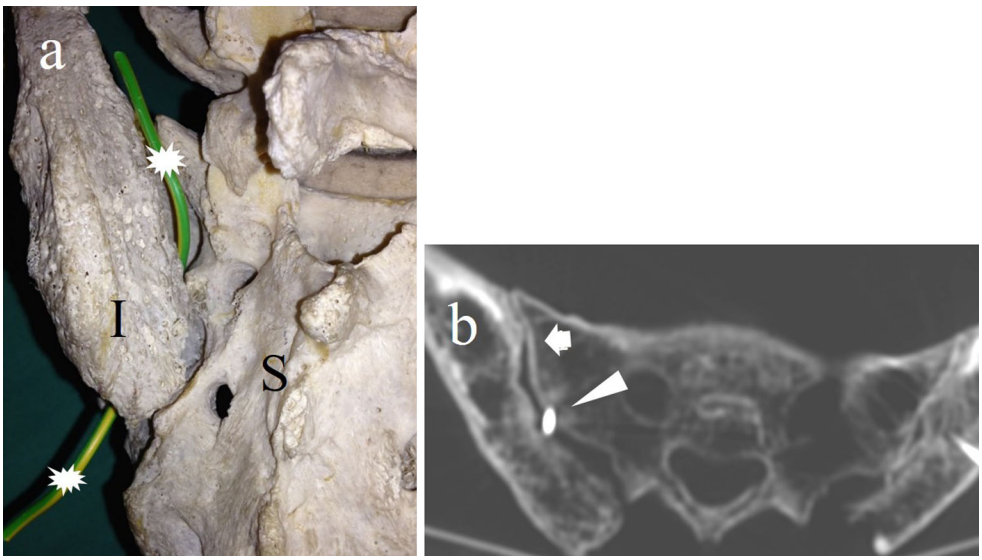


**Fig. 3** **a** Posterior aspect of the sacrum (S) and ilium (I) with a landmark (*asterisks*) introduced in the lowermost part of the cranial sacroiliac empty space, pushed down to exit just laterally to the second sacroiliac empty space. **b** Axial CT scan showing the landmark (*arrowhead*) located posteriorly to the S1 portion of the SIJ (*arrow*) in an extra-articular part of the sacroiliac region

## CT scanning of patients

The first coronal scan through the middle sacrum in which the upper three sacral foramens are visible and the interval between sacrum and ilium appears as a continuous space displays only the S1 and S3 portions of the SIJ (Fig. 4). The intermediate portion is an extra-articular part consisting of ilium with a flat, convex or concave medial outline. The S2 portion of SIJ can be visualized in the most anterior coronal scan, tangent to the anterior border of the sacral ala (Fig. 5).

Axial sections through the first sacral vertebra show the S1 portion of SIJ (Fig. 6a), similarly to those through the upper part of the first sacral foramen (Fig. 6b). At both

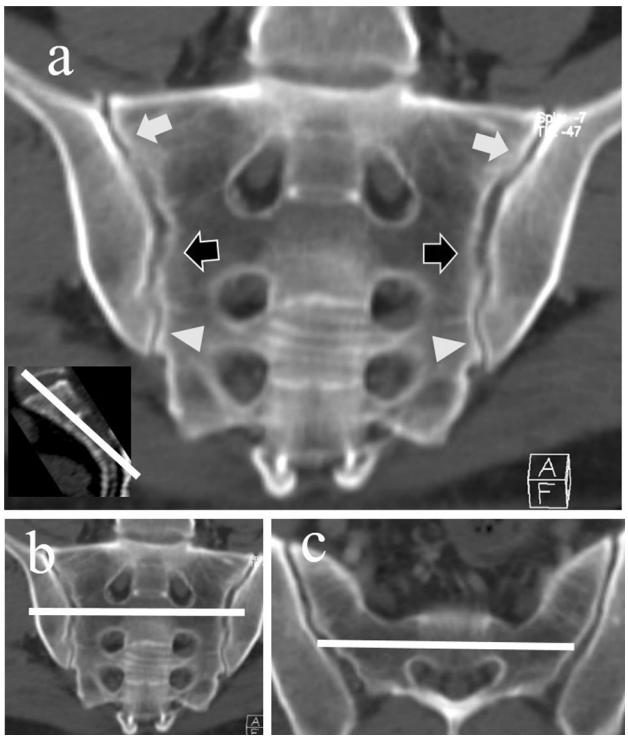


**Fig. 4** **a** Coronal CT scan showing the upper three sacral foramens and the interval between the ilium and sacrum, on each side, as a continuous, rather uniform, space; this section displays the S1 (*white arrows*) and S3 (*arrowheads*) portion of the SIJs, with intermediate extra-articular parts consisting of iliac bone (*black arrows*). The *insert* at the *left bottom* indicates the obliquity of the coronal image on the sagittal plane. **b**, **c** The *white lines* show the corresponding coronal and axial planes, respectively, of the image above

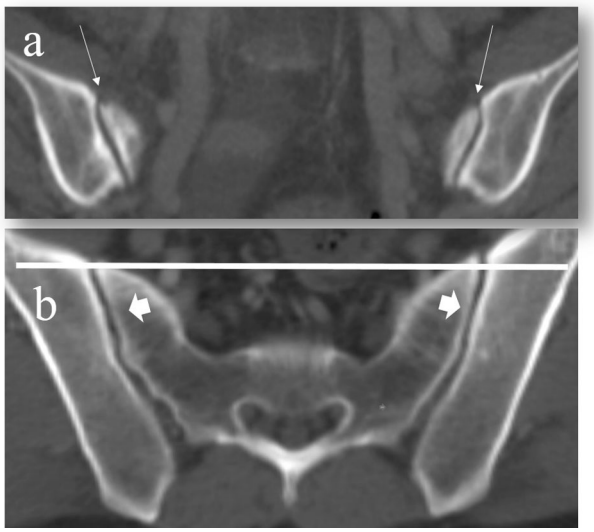


**Fig. 5** **a** Coronal image of the S2 portion of the SIJs (*arrows*) obtained on the plane tangent to the anterior border of the sacral ala. **b** The axial scan, with the *white line* indicating the corresponding plane (tangent to the anterior border of the SIJ) of the coronal image above, displays the S2 part of the SIJs (*arrows*), behind which large portions of extra-articular iliac bone are visible

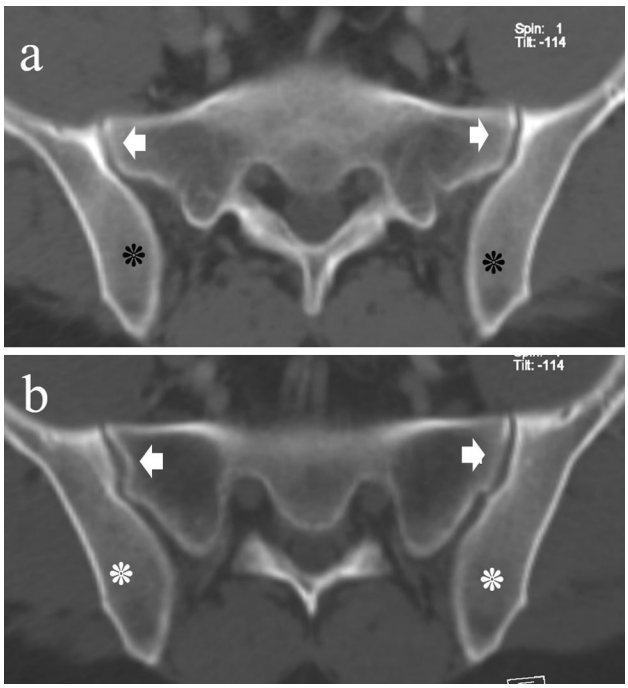


**Fig. 6** **a** Axial scan through the upper part of the S1 portion of the SIJs (*arrows*). **b** The axial scan obtained 6 mm below, through the first sacral foramen, shows a greater sagittal size of the joints (*arrows*). On both scans, posterolaterally to the S1 part of the SIJs, large portions of extra-articular iliac bone (*asterisks*) are visible, which extend beyond the first sacral vertebra

sites, the posterior parts of the sections show extra-articular portions consisting of iliac bone. Axial scans through the second sacral vertebra exhibit, anteriorly, the S2 portion of SIJ (Fig. 5b) and, posterolaterally, portions of ilium with variable features. The lowermost part of SIJ, located at the level of the lower S2, or uppermost S3, vertebra is a flat articular portion (Fig. 7). Its size is variable, but usually small.

A few patients exhibit the bone "variations" of the SIJ described in two studies [4, 19]. The so-called "iliosacral complex" is mostly found on axial scans through the S1 foramen as a marked prominence of the ilium towards a concavity of the lateral sacrum, i.e. clearly outside the SIJ (Fig. 8a). The "semicircular defect", usually visible at S2 level, consists of an indentation of the ilium facing a mild depression of the sacrum (Fig. 8b).

Measurement of JSW showed that in all age groups, including Group A, there were subjects with JSW $< 2$ mm, i.e., narrowing of articular space, at one or more sites on coronal and/or axial scans. However, with increasing age, the sites with normal JSW decreased and those with JSN increased (Table 2). In Group A, the mean JSW was $\geq 2$ mm on all eight (four on right and four on left side) S1 and S2 coronal or axial scans. In Group B, the mean JSW was normal in six of the eight sites, whereas in

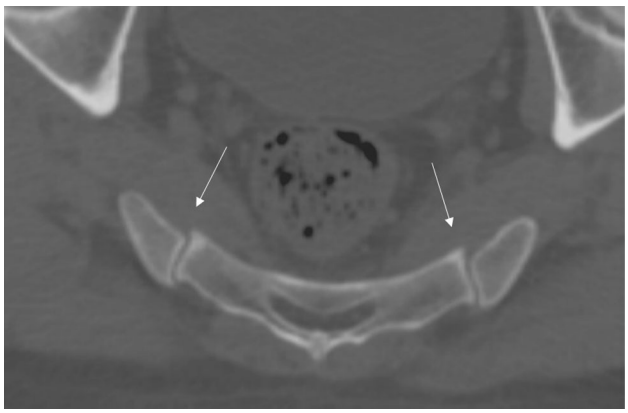

**Fig. 7** Axial scan showing the S3 portion of the SIJs (*thin arrows*), which is relatively large in this patient

Group C only the mean values of S1 coronal scans were normal. In Group D, the left S1 coronal scans had a normal mean width, whereas the others showed JSN. The S3 SIJ was consistently narrow in all groups. In 27 % of subjects the SIJ was fused, not measurable or apparently absent, mostly at S3 level.

## Discussion

Studies on the sacroiliac region have paid little attention to the extra-articular components that, instead, we found to be important for both strictly anatomical reasons and the interpretation of CT or MRI images of the sacroiliac

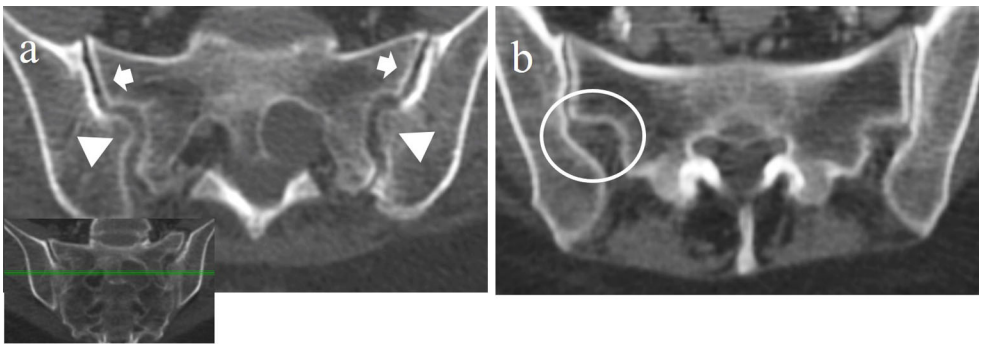


**Fig. 8** **a** Axial image of a 72-year-old osteoporotic female through the *upper* part of the first sacral foramens displaying, on both sides, a "iliosacral complex", consisting of a *marked* prominence of ilium (*arrowheads*) opposite to the cranial sacral depressions, behind the S1 portion of the SIJs (*arrows*); the *insert* shows the coronal scan at the corresponding level. **b** Axial scan at S2 level of a 47-year-old male exhibiting a "semicircular defect" (*encircled*) resulting from an indentation of the medial margin of the *right* ilium opposite to a depression of the lateral sacral border; a similar, less typical, image is present on the *left* side

**Table 2** Width (mm) of sacroiliac joint space on CT coronal and axial scans in groups of patients of different ages

| Age range (years) | 19–35 | | 36–50 | | 51–65 | | 66–82 | |
|---|---|---|---|---|---|---|---|---|
| Number of patients | $n = 20$ | | $n = 24$ | | $n = 23$ | | $n = 23$ | |
| Type of CT scan | Joint space width mean ± SD | | | | | | | |
| | Rt | Lt | Rt | Lt | Rt | Lt | Rt | Lt |
| Coronal | | | | | | | | |
| S1 | 2.23 ± 0.49 | 2.08 ± 0.32 | 2.2 ± 0.55 | 2.22 ± 0.3 | 2.01 ± 0.49 | 2.0 ± 0.2 | 1.98 ± 0.88 | 2.10 ± 0.83 |
| S2 | 2.0 ± 0.44 | 2.02 ± 0.38 | 2.0 ± 0.35 | 2.06 ± 0.82 | 1.94 ± 0.23 | 1.91 ± 0.44 | 1.87 ± 0.84 | 1.82 ± 0.81 |
| S3 | 1.74 ± 0.59 | 1.78 ± 0.31 | 1.67 ± 0.7 | 1.73 ± 0.39 | 1.72 ± 0.78 | 1.59 ± 0.86 | 1.68 ± 0.81 | 1.66 ± 0.61 |
| Axial | | | | | | | | |
| S1 | 2.09 ± 0.36 | 2.08 ± 0.5 | 2.26 ± 0.56 | 2.23 ± 0.51 | 1.90 ± 0.41 | 1.88 ± 0.21 | 1.95 ± 0.64 | 1.88 ± 0.8 |
| S2 | 2.01 ± 0.24 | 2.02 ± 0.28 | 1.90 ± 0.45 | 1.91 ± 0.27 | 1.92 ± 0.25 | 1.93 ± 0.39 | 1.82 ± 0.8 | 1.88 ± 0.74 |
| S3 | 1.92 ± 0.58 | 1.63 ± 0.28 | 1.75 ± 0.74 | 1.75 ± 0.5 | 1.61 ± 0.59 | 1.59 ± 0.8 | 1.57 ± 0.8 | 1.47 ± 0.58 |

*SD* standard deviation, *Rt* right side, *Lt* left side

region. The components which we refer to are the depressions situated on both sides of the posterior aspect of the sacrum and the extra-articular portion of the posteroinferior ilium that is in contact with those depressions to form extra-articular cavities in which the posterior sacroiliac ligaments insert. We found that both the sacral and iliac components have different morphometric features, even on the two sides of the same subject. Nevertheless, they adapt to each other to form the bony complex that allows the ilium to be connected to sacrum and the auricular surfaces to match each other.

The mechanical function of the SIJ is to allow the movements between the auricular surfaces of the sacrum and ilium, that have been named nutation (forward nodding) and counternutation (backward nodding), to be accomplished. A further function, however questioned [33], is a direct weight transfer from the axial to appendicular skeleton. This role is mainly played by the iliac tuberosity and the proximal bone prominence of sacrum which in vivo are in close contact with each other. This interpretation is consistent with the results of a study on the growth of human ilium showing that the extra-articular portion is considerably larger than the articular surface, a disparity that might be a response to the load placed on the extra-articular portion by the posterior sacroiliac ligaments [33].

Many CT studies [1, 2, 8, 11, 13, 14, 25, 28] show coronal images including the upper three sacral foramens as typical scans displaying the entire SIJ. We found these images to be misleading because they do not allow all articular portions to be visualized. They show the S1 and S3 parts of the SIJ, but not the S2 portion. On the coronal plane, the S2 portion is visible on the most ventral coronal scans due to the peculiar position and orientation of the SIJ. Its central part, in fact, is convex anteriorly and situated in a plane tangent to the anterior margin of the sacral ala, ventrally to the anterior, concave aspect of the middle part of the sacrum. This finding is important for correct assessment of the anatomy of both normal SIJ and that of patients with degenerative or inflammatory conditions.

In CT studies analyzing the age-related changes of SIJ in asymptomatic subjects, measurements of JSW along the interval between sacrum and ilium on coronal scans showing the upper three sacral foramens [8, 25, 28] may be erroneous, since these scans include articular and extra-articular components. The region between S1 and S3 portions of the joint, in fact, consists only of extra-articular ilium. Similarly, in CT studies of SIJ in rheumatic diseases, mostly based on coronal images, marginal erosions and bone sclerosis of the extra-articular portion, as well as JSN, may be mistaken for pathologic joint changes, as occurred in several studies [1, 2, 11, 13, 14], if the two parts are not clearly identified. Analogous considerations apply to MRI, widely used to assess conditions of rheumatic sacroiliitis, which are mostly evaluated on coronal scans showing the most cranial or all sacral foramens [9, 11, 17, 18, 26]. In MRI studies of inflammatory conditions, i.e. synovitis, the articular and extra-articular portions of the sacroiliac region have been termed anterior and posterior part of the SIJ, respectively [17, 18]. Thus, the term synovitis is used for areas with and without synovial tissue. This can generate confusion with other conditions, such as infections or tumors, which may display similar MRI features, but different locations in the sacroiliac region [11].

Almost none of previous CT studies in which the JSW was measured reported the levels where measurements were performed and whether they were made on both coronal and axial scans. In those studies, JSN was found in all age groups with figures ranging from 74 % [4] to 87 % [25]. In our cohort, measurements were performed at S1 to S3 levels and on coronal and axial scans in each subject. We found that until the age of 50 years few patients had JSN at S1 or S2 levels. Subsequently, the mean values of JSW were lower than in previous ages and more subjects had JSN, but even in the oldest patients, there were normal areas. These findings suggest that JSW is variable in different individuals due to both constitutional characteristics and degenerative changes, i.e. the JSW results from the original individual width and cartilage changes due to aging. Conversely, the joint space at S3 level was narrow at all ages and, in oldest patients, it was often fused or not identifiable, a finding that is consistent with our anatomical study showing that in a part of the sacra the caudal depression could not be identified.

Two variations of the SIJ described by Prassopoulos et al. [19] and Demir et al. [4] appear, indeed, peculiar features of the extra-articular portion of the sacroiliac region. The “iliosacral complex” is found behind the lower part of the S1 portion of the SIJ where the cranial, usually largest, sacral depression is located. It is seemingly due to the prominence of the ilium in front of that depression. The “semicircular defect”, mostly found at S2 level, is probably due to mild depression of the ilium in front of the middle sacral depression.

In recent years, patients with chronic SIJ pain often undergo joint fusion, mostly by percutaneous placement of triangle-shaped titanium implants or threaded screws across the SIJ, the operation being performed using fluoroscopy or navigation systems. A drawback of the procedure is the postoperative development of radiolucencsies around the implant or clear nonunion of the device [22, 31], that may occur when it is partly located in a non-osseous space between sacrum and ilium, for example in a semicircular defect not recognized on preoperative CT scans. A further drawback, more frequent and serious, is a complication caused by an implant or a screw placed into S1 or S2

foramen. In a cohort of 144 patients [23], there were 28 adverse events, of which 21 % were neural complications. Mason et al. [16], in a series of 73 patients, had two cases of immediate postoperative nerve pain, needing urgent re-operation. In a series of 50 cases [21], three patients with immediate postoperative radicular symptoms, in whom pelvic CT scanning showed implant misplacement, underwent revision surgery. Percutaneous sacroiliac fusion, although not extremely difficult, implies a fairly long learning curve. Surgeons using fluoroscopy need an exhaustive knowledge of the osseous anatomy as seen on fluoroscopic images, but also a good acquaintance of CT anatomy to identify preoperatively the morphology of their patients' sacroiliac region. For those using navigation systems it is important to have an adequate knowledge of the osseous anatomy but, especially, an excellent acquaintance of the CT anatomy of the region because what they see at surgery are CT images to which they must be well accustomed to carry out a rapid and uncomplicated operation.

## Conclusions

We first described the presence, on each side of the posterior aspect of the sacrum, of three depressions separated by bone prominences and analyzed the morphometry of the extra-articular portion of the posteroinferior part of the ilium, where the iliac tuberosity is located. When the ilium is connected to sacrum, the iliac tuberosity is in contact with the proximal sacral prominence to which it transfers the load of the upper part of the body. CT study showed that the coronal scan displaying the upper three sacral foramens, on which most studies on degenerative or inflammatory conditions are based, show only the S1 and S3 portions of the SIJ, the S2 portion being visible on the most anterior coronal scans. The joint space width results from both the constitutional characteristics of the subject and the age-related degenerative changes of the cartilage.

#### Compliance with ethical standards

**Ethical standards** All studies that we made comply with the current laws of the country in which they were performed.

**Conflict of interest** The authors have no conflict of interest to declare.

## References


1. Borlaza GS, Seigel R, Kuhns LR, Good AE, Rapp R, Martel W (1981) Computed tomography in the evaluation of sacroiliac arthritis. Radiology 139:437–444
2. Carrera GF, Foley WD, Kozin F, Ryan L, Lawson TL (1981) CT of sacroiliitis. AJR 136:41–46
3. Cheng JS, Song JK (2003) Anatomy of the sacrum. Neurosurg Focus 15:E3
4. Demir M, Mavi A, Gümüsburun E, Baytram M, Gürsoy S (2007) Anatomical variations with joint space measurement on CT. Kobe J Med Sci 53:209–217
5. Devauchelle-Pensec V, D'Agostino MA, Marion J, Lapierre M, Jousse-Joulin S, Colin D et al (2012) Computed tomography scanning facilitates the diagnosis of sacroiliitis in patients with suspected spondylarthritis: results of a prospective multicenter French cohort study. Arthritis Rheum 64:1412–1419. doi:10.1002/art.33466
6. Ehara S, El-Khoury GY, Bergman RA (1988) The accessory sacroiliac joint: a common anatomic variant. AJR 150:857–859
7. Elgafy H, Semaan HB, Ebraheim NA, Coombs RJ (2001) Computed tomography findings in patients with sacroiliac pain. Clin Orthop Relat Res 82:112–118
8. Faflia CP, Prassopoulos PK, Daskalogiannaki ME, Gourtsoyiannis NC (1998) Variation in the appearance of the normal sacroiliac joint on pelvic CT. Clin Radiol 53:742–746
9. Gaspersic N, Sersa I, Jevtic V, Tomsic M, Praprotnik S (2008) Monitoring ankylosing spondylitis therapy by dynamic contrast-enhanced and diffusion-weighted magnetic resonance imaging. Skeletal Radiol 37:123–131
10. Gray H (1918) Anatomy of human body. Lea & Febiger, Philadelphia
11. Guglielmi G, Cascavilla A, Scalzo G, Carotti M, Salaffi F, Grassi W (2011) Imaging findings of sacroiliac joints in spondyloarthropathies and other rheumatic conditions. Radiol Med 116:292–301. doi:10.1007/s11547-010-0607-z
12. Ha K-Y, Lee J-S, Kim K-W (2008) Degeneration of sacroiliac joint after instrumented lumbar or lumbosacral fusion. Spine 33:1192–1198. doi:10.1097/BRS.0b013e318170fd35
13. Kozin F, Carrera GF, Ryan LM, Foley D, Lawson T (1981) Computed tomography in the diagnosis of sacroiliitis. Arthritis Rheum 24:1479–1485
14. Lawson TL, Foley WD, Carrera GF, Berland LL (1982) The sacroiliac joints: anatomic, plain roentgenographic, and computed tomographic analysis. J Comput Assist Tomogr 6:307–314
15. Mahato NK (2010) Variable positions of the sacral auricular surface: classification and importance. Neurosurg Focus 28:E12
16. Mason LW, Chopra I, Mohanty K (2013) The percutaneous stabilisation of the sacroiliac joint with hollow modular anchorage screws: a prospective outcome study. Eur Spine J 22:2325–2331. doi:10.1007/s00586-013-2825-2
17. Muche B, Bollow M, François RJ, Sieper J, Hamm B, Braun J (2003) Anatomic structures involved in early- and late-stage sacroiliitis in spondylarthritis: a detailed analysis by contrast-enhanced magnetic resonance imaging. Arthritis Rheum 48:1374–1384
18. Prakash D, Prabhu SM, Irodi A (2014) Seronegative spondyloarthropathy-related sacroiliitis: CT, MRI features and differentials. Indian J Radiol Imaging 24:271–278. doi:10.4103/0971-3026.137046
19. Prassopoulos PK, Faflia CP, Voloudaki AE, Gourtsoyiannis NC (1999) Sacroiliac joints: anatomical variants on CT. J Comput Assist Tomogr 23:323–327
20. Renick D, Niwayama G, Goergen TG (1975) Degenerative disease of the sacroiliac joint. Invest Radiol 10:608–621
21. Rudolf L (2012) Sacroiliac joint arthrodesis-MIS technique with titanium implants: report of the first 50 patients and outcomes. Open Orthop J 6:495–502. Available via DIALOD. http://www.ncbi.nlm.nih.gov/pmc/articles/PMC3529399
22. Rudolf L, Capobianco R (2014) Five-year clinical and radiographic outcomes after minimally invasive sacroiliac joint fusion using triangular implants. Open Orthop J 8:375–383. doi: 10.

2174/1874325001206010495. Available via DIALOG. http://creativecommons.org/licenses/by-nc/3.0
23. Sachs D, Capobianco R, Cher D et al (2014) One-year outcomes after minimally invasive sacroiliac joint fusion with a series of triangular implants: a multicenter, patient-level analysis. Med Devices (Auckl) 7:299–304. Available via DIALOG. http://creativecommons.org/licenses/by-nc/3.0
24. Schünke M, Schulte E, Schumacher U (2011) Allgemeine Anatomie und Bewegungssystem, 3rd edn. Thieme Verlag, Stuttgart
25. Shibata Y, Shirai Y, Miyamoto M (2002) The aging process in the sacroiliac joint: helical computed tomography analysis. J Orthop Sci 7:712–718
26. Sudoł-Szopinska I, Urbanik A (2013) Diagnostic imaging of sacroiliac joints and the spine in the course of spondyloarthropathies Pol. J Radiol 78:43–49. doi:10.12659/PJR.889039
27. Testut L, Latarjet A (1948) Traité d'anatomie humaine. Nouvième édition revue par Latarjet A. Doin G and Cie, Paris
28. Vogler III Jr, Brown WH, Helms CA, Genant HK (1984) The normal sacroiliac joint: a CT study of asymptomatic patients. Radiology 151:433–437
29. Whelan MA, Gold RP (1982) Computed tomography of the sacrum: 1. Normal anatomy. AJR Am J Roentgenol 139:1183–1190
30. Williams PL (1995) Sacrum and lumbosacral joints. Gray's anatomy. Churchill Livingstone, London, pp 531–533
31. Wise CL, Dall BE (2008) Minimally invasive sacroiliac arthrodesis: outcomes of a new technique. J Spinal Disord Tech 21:579–584. doi:10.1097/BSD.0b013e31815ecc4b
32. Yagan R, Khan MA, Marmolya G (1987) Role of abdominal CT, when available in patients' records, in the evaluation of degenerative changes of the sacroiliac joints. Spine 12:1046–1051
33. Yusof NA, Soames RW, Cunningham CA, Black SM (2013) Growth of the human ilium: the anomalous sacroiliac junction. Anat Rec 296:1688–1694. doi:10.1002/ar.22785